NIH Public Access
Author Manuscript
Ann N Y Acad Sci. Author manuscript; available in PMC 2012 March 27.

Published in final edited form as:
Ann N Y Acad Sci. 2006 October ; 1080: 395–414. doi:10.1196/annals.1380.029.

Modeling Cardiac Ischemia

BLANCA RODRÍGUEZ[a], **NATALIA TRAYANOVA**[c], and **DENIS NOBLE**[b]

[a]Computing Laboratory, University of Oxford, Oxford OX1 3QD, UK [b]Department of Physiology, Anatomy and Genetics, University of Oxford, Oxford OX1 3PT, UK [c]Department of Biomedical Engineering, Johns Hopkins University, Baltimore, Maryland

Abstract

Myocardial ischemia is one of the main causes of sudden cardiac death, with 80% of victims suffering from coronary heart disease. In acute myocardial ischemia, the obstruction of coronary flow leads to the interruption of oxygen flow, glucose, and washout in the affected tissue. Cellular metabolism is impaired and severe electrophysiological changes in ionic currents and concentrations ensue, which favor the development of lethal cardiac arrhythmias such as ventricular fibrillation. Due to the burden imposed by ischemia in our societies, a large body of research has attempted to unravel the mechanisms of initiation, sustenance, and termination of cardiac arrhythmias in acute ischemia, but the rapidity and complexity of ischemia-induced changes as well as the limitations in current experimental techniques have hampered evaluation of ischemia-induced alterations in cardiac electrical activity and understanding of the underlying mechanisms. Over the last decade, computer simulations have demonstrated the ability to provide insight, with high spatiotemporal resolution, into ischemic abnormalities in cardiac electrophysiological behavior from the ionic channel to the whole organ. This article aims to review and summarize the results of these studies and to emphasize the role of computer simulations in improving the understanding of ischemia-related arrhythmias and how to efficiently terminate them.

Keywords

myocardial ischemia; computer simulations; cardiac arrhythmias; vulnerability to electric shocks

INTRODUCTION

Ventricular tachycardia and fibrillation are major causes of sudden cardiac death.[1,2] These arrhythmias arise from various clinical conditions, however, the foremost perpetrator among them is ischemic heart disease. Myocardial ischemic injury ensues from deficiencies in both energetic input and waste removal.[3] The result is progressive deterioration of electrical activity in the region of injury, leading to failure of contraction, and finally, cell death. At the organ level, this chain of events manifests itself ultimately as malignant arrhythmias and pump failure.[4]

The mechanisms underlying potentially lethal ventricular arrhythmias associated with ischemic cardiac disease are difficult to elucidate by clinical studies on patients who develop

© 2006 New York Academy of Sciences.

Address for correspondence: Dr. Blanca Rodríguez, Oxford University Computing Laboratory, Wolfson Building, Parks Road, Oxford, UK. Voice: +44-1865-283557; fax: +44-1865-273839. blanca@comlab.ox.ac.uk.

NIH-PA Author Manuscript
NIH-PA Author Manuscript
NIH-PA Author Manuscript

NIH-PA Author Manuscript

NIH-PA Author Manuscript

NIH-PA Author Manuscript

them; arrhythmias may occur before hospital admission, and even if occurring in the hospital setting, the primary concern is resuscitation and maintaining the patient's life, and not research in arrhythmogenesis. To study the electrophysiological changes associated with myocardial ischemic injury and how they lead to the establishment of ventricular tachycardia and fibrillation, animal models of clinical pathophysiology have been developed,[3,5] overcoming the limitations of clinical studies and playing an invaluable role in advancing mechanistic insight. Animal model studies have provided new ideas and hypotheses that have been tested in clinical studies and have thus increased the level of knowledge regarding arrhythmogenesis in the ischemic milieu.

Experimental models, however, have their own set of limitations that hamper the comprehensive evaluation of arrhythmogenic mechanisms, and thus the development of improved antiarrhythmia therapies to combat the consequences of ischemic cardiac disease. Electrophysiological changes following coronary occlusion are extremely rapid, particularly during the initial acute stage of ischemia (first 10-min postocclusion),[3] making it difficult to thoroughly assess the cause-and-effect relations between metabolic and electrophysiological parameters. In addition, current experimental techniques for recording electrical behavior at the tissue and organ level are limited in their ability to document, with sufficient spatial resolution, events confined within the depths of the ventricular wall.

Over the last decade, analysis of electrophysiological phenomena has been significantly augmented and advanced by the use of mathematical modeling and computer simulations, from the ionic channel to the whole organ. One of the major contributions of computational research in electrophysiology has been the ability of mathematical models to dissect various effects and to tease out important relations between electrophysiological parameters. This effort has been particularly important in ascertaining the role of ischemic abnormalities in cardiac electrophysiological behavior. The purpose of this article is to briefly review some of the computational models, from ionic fluxes to whole-heart behavior, which have been used to elucidate (1) the electrophysiological consequences of ischemic injury, (2) the mechanisms that underlie arrhythmia generation under the conditions of ischemia, and (3) how defibrillation works in the ischemic heart. The review focuses on modeling and simulation representing events during the initial acute phase of ischemic injury, phase 1A, since it constitutes the most rapid and difficult to analyze phase of ischemic cardiac disease.

Alterations in Metabolism and Ionic Concentrations in Ischemia

Membrane ionic transporters are sensitive to intracellular and extracellular ions and metabolites. It is through these interactions that metabolic changes in ischemia exert their electrophysiological effects.[3] Large changes in these parameters in ischemia have been measured experimentally, including increased concentrations of intracellular Na^+ and Ca^{2+}, increased extracellular K^+, decreased extracellular Na^+, and decreased intracellular ATP and pH. Arrhythmias under the conditions of myocardial ischemia are therefore multifactor pathologies. One of the earliest attempts to simulate arrhythmic mechanisms linked to ischemia was made by Ch'en *et al*.[6] who succeeded in connecting Na^+/Ca^+ overload during ATP depletion and intracellular acidity to oscillations of internal Ca^{2+} that could be the trigger of some forms of arrhythmia. Their modeling of metabolism was, however, limited to ATP depletion and fall in pH. More extensive models now exist.

Zhou *et al*.[7] have modeled both the transport and metabolism of various chemical species, including blood-interstitial fluid, cytosolic and mitochondrial compartments as well as a glycolytic subdomain in the cytosol. The model successfully simulated the activation of glycogen breakdown and the switch to lactate production induced by reduced blood flow in an *in vivo* experimental system. Cabrera *et al*.[8] have described a mathematical model of myocardial energy metabolism that was used to investigate the role of cytosolic and

NIH-PA Author Manuscript

NIH-PA Author Manuscript

NIH-PA Author Manuscript

mitochondrial redox states in regulating cardiac energetics during reduced myocardial blood flow.

One of the controversial questions in this field is the function of Na^+/Ca^{2+} exchange, with some studies proposing that the exchanger reverses direction in ischemia. That it does so transiently is not in doubt, but long-term reversal seems unlikely, since this would always create precisely those changes in ion concentrations required to revert to forward mode. Computations done with a simplified form of the Ch'en *et al*. model show that this view is consistent with the experimental data provided that a substantial fall in interstitial Na^+ occurs.[9] Unraveling the impact of Na^+/Ca^{2+} exchange in ischemia is difficult since it plays more than one role. Under normal circumstances, the exchanger is the main route for Ca^{2+} efflux, accounting for up to 90% of this flux.[10] But it also carries ionic current, which in the forward mode is inward, meaning that it is capable of causing ectopic excitations. Despite carrying the great majority of Ca^{2+} efflux in normal electrical activity, knockout of 80–90% of the Na^+/Ca^{2+} exchanger in mice leaves functional cardiac cells.[11] Clearly, other transporter mechanisms, in particular the sarcolemmal Ca^{2+} pump, can take over. The implications of these results for the study of ischemia have yet to be explored. In an important study, Imahashi *et al*.[12] have shown that cardiac specific ablation of the Na^+/Ca^{2+} exchanger confers protection against ischemia and reperfusion injury, although they also conclude that the rise in intracellular sodium is not itself a major factor determining injury.

Changes in interstitial ion concentrations have been highlighted in the work of Rodríguez *et al*.,[13] with a focus on the mechanisms of extracellular K^+ accumulation in ischemia. Extracellular K^+ concentration ($[K^+]_o$) is known to increase very quickly following coronary occlusion, reaching a plateau level of 6–11 mmol/L above its normal value at 10–15 min postocclusion.[14–20] The increase in $[K^+]_o$ is one of the major contributors to the genesis and sustenance of ischemia-related cardiac arrhythmias,[4] and thus a large body of research has been devoted to the mechanisms of extracellular K^+ accumulation in ischemia. However, this daunting task requires gathering information on ischemia-induced alterations in all ionic currents and concentrations and in the transmembrane potential simultaneously, which is next to impossible using current experimental techniques. Rodríguez *et al*.[13] used a computer model of a single cardiomyocyte to dynamically calculate ionic concentrations and fluxes under ischemic conditions with the aim of providing mechanistic insight into the extracellular K^+ accumulation in ischemia. The model considered ionic fluxes between three compartments: the intracellular medium, the interstitial cleft, and the bulk extracellular medium, in which concentrations were assumed to be constant. Membrane kinetics were represented by a modified version of the Luo–Rudy action potential (AP) model[21,22] that includes a formulation of the ATP-sensitive K^+ current ($I_{K(ATP)}$) current by Ferrero *et al*.[23] and a new ischemia-activated Na^+ current (I_{NaS}). Interruption of coronary flow was simulated by steeply increasing the time constant of diffusion between the bulk extracellular medium and the interstitial clefts from its normoxic value to infinity. Experimental results suggest that three mechanisms, namely inhibition of the Na^+/K^+ pump (I_{NaK}),[24,25] activation of the $I_{K(ATP)}$,[18,26] and activation of an inward Na^+ current[18,27–29] could be responsible for the increase in $[K^+]_o$ in acute ischemia. Rodríguez *et al*.[13] conducted computer simulations to investigate the role of each of these three mechanisms in extracellular K^+ accumulation during the early phase of ischemia.

Figure 1 summarizes the main results of the simulations, which ascertain that the simultaneous participation of the three mechanisms (Trace VII) is necessary to obtain the biphasic (quick rise and then plateau phase) increase in $[K^+]_o$ observed experimentally during the first 10–15 min following interruption of coronary flow. Engagement of only one (Traces I–III) or two (Traces IV–VI) of these mechanisms cannot explain the extracellular K^+ accumulation recorded experimentally: the increase in $[K^+]_o$ is either too low as

NIH-PA Author Manuscript

NIH-PA Author Manuscript

NIH-PA Author Manuscript

compared to experimental data or does not replicate the biphasic increase. The simulation results also demonstrate that the rate of activation of the three mechanisms as well as the rate at which the cell is paced determine the level and the time to onset of the $[K^+]_o$ plateau phase, consistent with experimental recordings.[15,17–19,30] Acidosis and ischemic shrinkage of the extracellular space[3,20,31] have a minor effect on the ischemic increase in $[K^+]_o$ and only produce a slight anticipation in time of the $[K^+]_o$ plateau phase. According to the simulation results, the ischemic cellular K^+ loss is mainly due to an increase in the K^+ efflux via the time-independent K^+ current and the $I_{K(ATP)}$, rather than to a decrease in K^+ influx via the Na^+/K^+ pump. The insight provided by these simulations is an important stepping stone in understanding the pathophysiology of ischemic injury in the heart.

Ischemia-Induced Changes in Action Potential and Propagation

Over the last four decades, increasing wealth in experimental data on ionic channel behavior has prompted its integration into highly sophisticated data-driven mathematical models of cardiac cell membrane kinetics, including representations of the ischemic milieu. Computer simulations with such models have improved significantly the understanding of the ionic mechanisms underlying ischemia-induced electrophysiological changes at the cellular and tissue level. Figure 2 illustrates a simulation of the evolution of ventricular cell AP over the first 12 min following coronary occlusion. Ischemia was simulated by incorporating effects of hyperkalemia, acidosis, and anoxia.[32,33] Specifically, the $[K^+]_o$ was increased from its normal value, 5.4 mmol/L, to 12 mmol/L;[15,34] the maximum conductances of the Na^+ and L-Type Ca^{2+} channels (currents I_{Na} and I_{CaL}, respectively) were decreased by 25%, representing inhibition by acidosis;[35–37] and the $I_{K(ATP)}$ was activated by decreasing the intracellular ATP concentration from 6.8 mmol/L to 4.6 mmol/L and increasing the intracellular ADP concentration from 15 μmol/L to 99 μmol/L.[23,34] Shaw and Rudy[38,39] and Ferrero *et al*.[23] demonstrated using computer simulations that these changes account for the most significant alterations in AP morphology and wave propagation over the course of ischemia. Indeed, Figure 2 shows that during the first 12 min of ischemia, resting potential becomes elevated to −60mV from its normal value of −85 mV, action potential duration shortens by almost 50% of its normal value, and the action potential amplitude progressively decreases from 125 mV to 88 mV. These changes are consistent with experimental recordings.[3,15,34,40]

The high degree of electrophysiological detail provided by computer simulations allows examination of the specific contribution of each ischemic change at the ionic level to the electrophysiological alterations in AP and propagation following coronary occlusion. For instance, computer simulation studies have shown that activation of a small portion of the K(ATP) channels is responsible for the significant action potential duration (APD) shortening observed in anoxic cardiomyocytes, while increase in $[K^+]_o$ plays only a secondary role in APD shortening.[23,38] The main effect of $[K^+]_o$ elevation is resting depolarization, which causes decreased availability of Na^+ channels and slow recovery of the Na^+ channel inactivation gates, thus resulting in depressed excitability and prolonged postrepolarization refractoriness in ischemic cardiomyocytes.[38] Excitability of ischemic myocytes is further reduced by acidosis that acts to decrease the maximum conductances of the Na^+ and Ca^{2+} channels.

As demonstrated by computer simulations and experimental studies, ischemia-induced alterations in Na^+ and Ca^{2+} currents have a significant impact on the AP upstroke, thus affecting propagation velocity. During the first minutes of ischemia, mild elevation of resting potential due to an initial increase in $[K^+]_o$ to around 8 mM leads to a decrease in the difference between resting potential and the threshold for activation, resulting in a slight increase in conduction velocity.[39,41,42] With further progression of ischemia, and further increase in $[K^+]_o$ above 8mM, severe depolarization at rest results in reduced availability of

NIH-PA Author Manuscript

NIH-PA Author Manuscript

NIH-PA Author Manuscript

Na^+ current and thus in slow AP upstroke and decreased propagation velocity.[39,41,42] While under normal conditions and in mild ischemia the AP upstroke velocity is mainly determined by the Na^+ current, under severe ischemic conditions (10–12-min postocclusion), the AP upstroke becomes biphasic, with the first phase corresponding to the influx of (decreased) Na^+ current and the second component due to the activation of the Ca^{2+} current.[39,43–47] Simulation studies have demonstrated that, under these conditions, Ca^{2+} current plays a critical role in the occurrence of propagation block and the development of alternans in the ischemic region, both phenomena being precursors of reentrant activity in ischemia.[39,47–49]

Ischemia-Induced Changes in the Electrocardiogram (ECG)

ECG ST-segment depression is recognized clinically as a sign of myocardial ischemia,[50,51] but the underlying mechanisms remain controversial. A number of studies have used computer simulations to investigate the role of specific features of the ischemic region, such as its location, in ST-segment displacement, in an attempt to ascertain the diagnostic value of the latter. Li *et al*.[52] investigated the origin of ST depression in the ECG for subendocardial ischemia by mapping the epicardial and endocardial potential distribution in *in vivo* sheep heart and by conducting computer simulations using a geometrically realistic passive model of the human heart. The results showed that ST depression was caused by an "injury current" generated by a spatial gradient in transmembrane potential at the border between ischemic and healthy tissue. As subendocardial ischemia progressed to full-thickness transmural ischemia, epicardial ST depression over the boundary region gradually increased, and ST elevation took place over the ischemic region. However, the location of the ischemic region in the ventricles could not be predicted by the ST depression on the epicardium.

The computer model by Li *et al*.,[52] while anatomically based, did not incorporate anisotropic conductivities. Follow-up work by the same group[53,54] and research by others[55–58] employed passive bidomain models to investigate how the anisotropic myocardial conductivities modulate the ST segment shift resulting from subendocardial ischemia. Results show that fiber rotation and tissue anisotropy play a key role in determining epicardial potential distributions and ST displacements in regional ischemia. However, these studies have an important limitation—the use of steady-state passive models, in which ischemia-induced alterations in membrane kinetics are not represented; such models cannot provide insight into the ionic basis of ischemia-induced alterations in the ECG in its entirety (and not only in ST segment shifts).

Gima and Rudy[59] and later Aslanidi *et al*.[60] adopted an alternative approach to investigate the cellular mechanisms underlying ischemia-induced changes in the ECG. They used a geometrically simple but electrophysiologically detailed 1D model of a virtual ventricular wall to compute the pseudo-ECG in normoxia and under conditions of global and subendocardial ischemia. Consistent with clinical and experimental data, the simulations showed that propagation through the ventricular wall results in an ST-segment at base line in normoxia, ST-segment elevation in global ischemia, and ST-segment depression in subendocardial ischemia caused by the abnormal transmural sequence of repolarization and resting potential elevation in the ischemic tissue.

Ischemia-Related Cardiac Arrhythmias

Ischemic impact on the myocardium is characterized with a high degree of heterogeneity. Electrophysiological properties vary not only with time post-occlusion, but also spatially. Due to diffusion of ions and metabolites, the core of the tissue suffering from a lack of flow, that is the central ischemic zone (CIZ), is surrounded by border zones (BZ), which comprise

NIH-PA Author Manuscript

NIH-PA Author Manuscript

NIH-PA Author Manuscript

progressive changes in electrophysiological properties between the healthy and ischemic regions. Experimental measurements of $[K^+]_o$, oxygen, and metabolite distribution in the ischemic area[61–65] were used by Ferrero *et al*.[47] to develop the 2D model of regional ischemia depicted in Figure 3A, which included the first electrophysiologically detailed model of the BZ. As in previous studies, ischemia was represented by the effects of hyperkalemia, acidosis, and hypoxia on $[K^+]_o$, I_{Na}, I_{CaL}, and $I_{K(ATP)}$, at levels corresponding to 10-min postocclusion. Severity of ischemic changes is most pronounced within the CIZ and decreases progressively in the BZ. The varying levels of $[K^+]_o$, I_{Na}, I_{CaL}, and $I_{K(ATP)}$ in the ischemic region result in a significant dispersion of refractoriness and of conduction velocity by the mechanisms explained in the previous section. Figure 3B shows the spatial variation of conduction velocity, APD, and effective refractory period in the border zone, as quantified by Ferrero *et al.*[47]

Dispersion of refractoriness and of conduction velocity in regional ischemia provides the substrate for the establishment of reentrant circuits, the main mechanism of arrhythmogenesis following coronary occlusion.[45,46,63] Figure 3C illustrates the initiation of a figure-of-eight reentry in the model of regional ischemia described above. Following pacing stimulation, a premature stimulus is applied at the bottom border of the 2D sheet. The premature stimulus elicits a wavefront, which propagates through the healthy region as well as the BZs, but blocks at the CIZ where refractoriness is extended. Meanwhile, tissue in the CIZ recovers allowing reentry of the wavefront from the top, and the establishment of a figure-of-eight reentrant circuit, a pattern similar to the one observed experimentally.[66–69] Simulation results show that the degree of activation of the $I_{K(ATP)}$ plays an important role in vulnerability to reentry in regional ischemia.[47,70]

The occlusion of a coronary artery leads to important electrophysiological heterogeneities, not only intramurally as represented in the model developed by Ferrero *et al*., but also transmurally, in the depth of the ventricular wall. A thin layer of tissue, approximately 1–2 mm, on both epi- and endocardium, receives nutrients and oxygen from blood in the cavities and the medium surrounding the heart, thus remaining viable over the course of acute ischemia.[71] In addition, the severity of ischemic changes varies transmurally through the core of the ischemic region. Extracellular K^+ accumulation is faster in the subendocardium than in the subepicardium while APD shortening due to $I_{K(ATP)}$ activation is more pronounced in the subepicardium, thus leading to gradients in the electrophysiological properties within the central ischemic region.[72–76]

The contribution of transmural electrophysiological heterogeneities in the is-chemic region to arrhythmogenesis in acute ischemia remains unknown due to limitations in current experimental techniques, which prevent the examination of cardiac activity in the depth of the ventricular wall with high spatial and temporal resolution. Recently, Tice *et al*.[48] developed an anatomically based 2D model of a transmural section of the ischemic rabbit ventricles following LAD occlusion. The model was used to investigate the role of regional ischemia-induced transmural heterogeneities in providing the substrate for reentry over the course of the first 10-min postocclusion. Ischemic substrate was represented by progressive changes in membrane dynamics due to hyperkalemia, acidosis, and hypoxia corresponding to 2–10-min postocclusion. The model, illustrated in Figure 4A, includes realistic CIZ, lateral BZ, endocardial and epicardial BZ (EBZ), and transmural I_{KATP} and $[K^+]_o$ gradients in CIZ. The LV wall was paced at 200 msec basic cycle length and premature stimulation was applied to the RV endocardium at a range of coupling intervals (CIs). The simulation results show that a premature stimulus is more likely to initiate arrhythmia at 7–8-min postocclusion, when refractoriness in normal tissue and CIZ differs the most. Arrhythmia induction is then heralded by alternans in the EBZ, as shown in Figure 4B. Within the vulnerable window (VW), propagation induced by the premature stimulus encounters

NIH-PA Author Manuscript

NIH-PA Author Manuscript

NIH-PA Author Manuscript

refractory RV and CIZ, while tissue in the EBZs is already recovered, resulting in reentry (Fig. 4B). Halving EBZ decreases the safety factor for propagation, resulting in 58.8% decrease in reentry initiation. Omission of transmural CIZ I_{KATP} gradient from the model causes 29.4% increase in probability of arrhythmia initiation due to greater difference in normal versus CIZ refractoriness. These simulation results provide an important mechanistic insight into the role of electrophysiological heterogeneities to arrhythmogenesis in regional ischemia.

Response of Ischemic Tissue to Electric Shocks

The only effective therapy currently available to terminate lethal cardiac arrhythmias arising from ischemic injury is electrical defibrillation by timely application of an electric shock. Due to the strong link between defibrillation threshold and upper limit of vulnerability (ULV),[77–79] numerous studies have investigated the mechanisms of cardiac vulnerability to electric shocks in an attempt to understand defibrillation failure. However, the majority of these studies focused on healthy ventricles[80–89] and rarely on hearts with ischemic disease,[90] thus little is known about the response of ischemic tissue to the application of electric shocks. This is in part due to the fact that experimental evaluation of shock-induced responses of ischemic tissue is hampered by the rapidity and complexity of ischemic changes that follow coronary occlusion.

Bidomain simulations have demonstrated ability to provide insight, based on behavior monitored with high spatiotemporal resolution, into the mechanisms of cardiac defibrillation in the healthy and ischemic ventricles.[41,42,81,84–86] The bidomain model[87] represents the myocardium as two coupled continuous media, the intracellular and the extracellular spaces, and allows for the study of the macroscopic tissue response to electric stimuli. As shown by experimental[88–93] and bidomain simulation studies,[82,83,94,95] the application of a strong electric field to the myocardium induces positive and negative changes in transmembrane potential, and results in large-scale regions of positive and negative membrane polarization termed virtual electrode polarization (VEP). Regions negatively polarized at shock end represent new excitable areas through which postshock wavefronts will propagate. The positively polarized regions play the dual role of first providing the electrical stimulus necessary for initiation of postshock propagating wavefronts and second being regions of immediate postshock refractoriness that could result in propagation block.

Tissue is vulnerable to an electric shock if postshock propagation results in reentry, which implies the fulfillment of three conditions: (1) new excitations have to be generated at the end of the shock at the borders of oppositely polarized areas; (2) postshock refractoriness in the positively polarized regions has to be long enough to result in propagation block in part of the ventricles; (3) the spatial extent of postshock wavefronts and their propagation velocity has to be such that tissue depolarized by the shock recovers before the postshock excitable areas have been completely consumed by postshock wavefronts.

Bidomain simulations using anatomically based finite element models have shown how these three factors manifest themselves in the 3D volume of the normal and the globally ischemic ventricles.[41,81,85] As in previous studies, changes in membrane dynamics over the course of the first 10 min following occlusion were implemented via the effects of hyperkalemia, acidosis, and hypoxia at the ionic level. To examine vulnerability to electric shocks in global ischemia, in the study by Rodríguez *et al.*,[41] three representative levels of increasing severity within the first 10-min interval were singled out. Simulations were conducted in normoxia and for each ischemic state to determine changes in cardiac vulnerability to electric shocks over the course of ischemia. To do so, the ventricles were paced at the apex and monophasic shocks of several strengths were applied at different CIs via two planar electrodes located at the boundaries of the perfusing bath to determine the

NIH-PA Author Manuscript

NIH-PA Author Manuscript

NIH-PA Author Manuscript

vulnerability grids, that is, 2D grids encompassing the episodes of shock-induced arrhythmogenesis. The ULV was determined in normoxia and over the course of ischemia as the lowest shock strength above which no sustained arrhythmia was induced.

Consistent with experimental results,[81] the simulations showed that the application of an external shock induces two main areas of opposite-in-sign polarization in both the normoxic and the globally ischemic ventricles (see Fig. 5: 0 ms panel). In both normoxia and ischemia, following shocks below the ULV, a new wavefront arises at shock end at the apex, proceeding toward the base through the shock-induced excitable gap in the LV. Meanwhile, shock-induced refractoriness in the RV-free wall causes a transient unidirectional block. Thus, while LV and septal tissue is being depolarized by wavefront propagation, the RV myocardium recovers, providing the return pathway for reentry (Fig. 5).

While the same type of reentrant pattern is induced in normoxia and in global ischemia, important differences in the characteristics of the postshock wavefronts and in their propagation develop over the course of global ischemia phase 1A; these differences result in a decrease in the ULV at around 4–5 min following the interruption of coronary flow. As described above, action potential duration is significantly shorter at 4–5 min of ischemia as compared to normoxia, resulting in shorter repolarization times and in an increase in the amount of tissue repolarized at a given CI (Fig. 5, preshock panel). As a consequence of these changes, the spatial extent of shock-end wavefronts increases in global ischemia as compared to normoxia. Larger wavefronts traverse the postshock excitable gap faster for the same shock strength, thus increasing the likelihood of wavefronts being blocked by the prolonged refractoriness in positively polarized areas immediately after shock end, and resulting in a decrease in ULV from its normal value of 12.75 V/cm to 9.6 V/cm at 4–5 min of global ischemia.

As ischemia progresses, APD shortening continues, however, resting potential elevation becomes more severe, causing prolonged postrepolarization refractoriness. As stated above, the APD shortening in ischemia results in an increase in the amount of tissue repolarized at a given CI. However, in the late stages of ischemia phase 1A, some of the tissue experiences low postshock excitability due to delay in the recovery of the Na inactivation gates caused by resting potential elevation. Since the ventricles are paced at the apex, the apical regions are always more recovered than the rest of the ventricles. Therefore, in the late stages of ischemia, postshock activations manage to traverse the apical regions, only to become decremental and to fail in the less-recovered basal portions (Fig. 5), thus resulting in a further decrease in cardiac vulnerability to electric shocks. At the end of ischemia phase 1A, no arrhythmia or even a single extra beat can be induced, regardless of CI or shock strength.[42] For all combinations of shock strength and CI, propagation initiated at shock end terminates shortly thereafter due to conduction failure. These fascinating results clearly underscore the utility of 3D realistic modeling in providing novel information regarding the electrical behavior of the heart under ischemic conditions as well as its response to antiarrhythmia therapy.

SUMMARY

This article provided a brief review of some of the computational models, from models of ionic fluxes to those of the whole organ, used to assess the electrophysiological effects of acute myocardial ischemia in its most rapid phase, 1A. It focused on alterations in metabolism and ionic fluxes; the changes in the cell AP morphology and its propagation; the manifestation of ischemia in the ECG; the mechanisms of arrhythmia generation; and the responses of the ischemic heart to electric shocks. The selection of topics included here is (necessarily) incomplete, but provides a mosaic of a variety of simulation approaches that

NIH-PA Author Manuscript

NIH-PA Author Manuscript

NIH-PA Author Manuscript

have addressed different aspects of the big picture. The review emphasized the fact that computer simulations are capable of providing mechanistic insight at any level of structural complexity. The article also provided an overview of the development of computer models of ever-increasing ionic and structural detail; models are now available from the single channel and cell level to the entire organ. Whole organ models that incorporate detailed ionic representation of the impact of ischemic injury are now becoming state-of-the-art[96] and hold the promise to lead to a breakthrough in understanding the arrhythmogenic mechanisms of myocardial ischemia and ultimately, in advancement of antiarrhythmia therapies.

Acknowledgments

This work was supported by the EPSRC-funded Integrative Biology e-Science pilot project (ref no: GR/S72023/01), by the EU BioSim Grant (005137) and by AHA Established Investigator Award (N.T.), and the grant HL63195 from NIH (N.T.). The authors would like to thank Drs. Jose María Ferrero, Jr., and Beatriz Trénor (Universidad Politécnica de Valencia), and Mr. Brock Tice (Tulane University) for helpful comments and for material provided for the figures.

References

1. Zipes DP, Wellens HJJ. Sudden cardiac death. Circulation. 1998; 98:2334–2351. [PubMed: 9826323]
2. Rubart M, Zipes DP. Mechanisms of sudden cardiac death. J Clin Invest. 2005; 115:2305–2315. [PubMed: 16138184]
3. Carmeliet E. Cardiac ionic currents and acute ischemia: from channels to arrhythmias. Physiol Rev. 1999; 79:917–1017. [PubMed: 10390520]
4. Harris AS, Bisteni A, Russell RA, et al. Excitatory factors in ventricular tachycardia resulting from myocardial ischemia. Potassium a major excitant. Science. 1954; 119:200–203. [PubMed: 13135509]
5. Wit AL, Janse MJ. Experimental models of ventricular tachycardia and fibrillation caused by ischemia and infarction. Circulation. 1992; 85(Suppl I):I32–I42. [PubMed: 1728503]
6. Ch'en FF, Vaughan-Jones RD, Clarke K, Noble D. Modelling myocardial ischaemia and reperfusion. Prog Biophys Mol Biol. 1998; 69:515–538. [PubMed: 9785954]
7. Zhou L, Salem JE, Saidel GM, et al. Mechanistic model of cardiac energy metabolism predicts localization of glycolysis to cytosolic subdomain during ischemia. Am J Physiol Heart Circ Physiol. 2005; 288:H2400–H2411. [PubMed: 15681693]
8. Cabrera ME, Zhou L, Stanley WC, Saidel GM. Regulation of cardiac energetics: role of redox state and cellular compartmentation during ischemia. Ann N Y Acad Sci. 2005; 1047:259–270. [PubMed: 16093502]
9. Noble D. Simulation of Na-Ca exchange activity during ischemia. Ann N Y Acad Sci. 2002; 976:431–437. [PubMed: 12502592]
10. Eisner DA, Sipido KR. Sodium calcium exchange in the heart. Necessity or Luxury? Circ Res. 2004; 95:549–551. [PubMed: 15375019]
11. Henderson SA, Goldhaber JI, So JM, et al. Functional adult myocardium in the absence of Na^+-Ca^{2+} exchange: cardiac specific knockout of NCX1. Circ Res. 2004; 95:604–611. [PubMed: 15308581]
12. Imahashi K, Pott C, Goldhaberi J, et al. Cardiac-specific ablation of the Na^+-Ca^{2+} exchanger confers protection against ischemia/reperfusion injury. Circ Res. 2005; 97:916–921. [PubMed: 16179590]
13. Rodríguez B, Ferrero JM Jr, Trenor B. Mechanistic investigation of extracellular K^+ accumulation during acute myocardial ischemia. Am J Physiol. 2002; 283:H490–H500.
14. Gasser RNA, Vaughan-Jones RD. Mechanism of potassium efflux and action potential shortening during ischaemia in isolated mammalian cardiac muscle. J Physiol. 1990; 431:713–741. [PubMed: 2129231]

NIH-PA Author Manuscript

NIH-PA Author Manuscript

NIH-PA Author Manuscript

15. Weiss JN, Shine KI. $[K^+]_o$ accumulation and electrophysiological alterations during early myocardial ischemia. Am J Physiol Heart Circ Physiol. 1982; 243:H318–H327.
16. Weiss JN, Shine KI. Extracellular K^+ accumulation during myocardial ischemia in isolated rabbit heart. Am J Physiol Heart Circ Physiol. 1982; 242:H619–H628.
17. Weiss JN, Shine KI. Effects of heart rate on extracellular K^+ accumulation during myocardial ischemia. Am J Physiol Heart Circ Physiol. 1986; 250:H982–H991.
18. Wilde AAM, Aksnes G. Myocardial potassium loss and cell depolarization in ischaemia and hypoxia. Cardiovasc Res. 1995; 29:1–15. [PubMed: 7895226]
19. Wilde AAM, Escande D, Schumacher CA, et al. Potassium accumulation in the globally ischaemic mammalian heart: a role for the ATP-sensitive K channel. Circ Res. 1990; 67:835–843. [PubMed: 2119912]
20. Yan GX, Chen J, Yamada KA, et al. Contribution of shrinkage of extracellular space to extracellular K+ accumulation in myocardial ischemia of the rabbit. J Physiol. 1996; 490:215–228. [PubMed: 8745289]
21. Luo CH, Rudy Y. A dynamic model of the cardiac ventricular action potential. I. Simulations of ionic currents and concentration changes. Circ Res. 1994; 74:1071–1096. [PubMed: 7514509]
22. Zeng J, Laurita KR, Rosenbaum DS, Rudy Y. Two components of the delayed rectifier K^+ current in ventricular myocytes of the guinea-pig type: theoretical formulation and their role in repolarization. Circ Res. 1995; 77:140–152. [PubMed: 7788872]
23. Ferrero JM Jr, Saiz J, Ferrero JM, Thakor NV. Simulation of action potentials from metabolically impaired cardiac myocytes. Role of ATP-sensitive K^+ current. Circ Res. 1996; 79:208–221. [PubMed: 8755997]
24. Wilde AAM, Peters RLG, Janse MJ. Catecholamine release and potassium accumulation in the isolated globally ischemic rabbit heart. J Mol Cell Cardiol. 1988; 20:887–896. [PubMed: 3216399]
25. Bersohn MM, Philipson KD, Fukushima JY. Sodium–calcium exchange and sarcolemmal enzymes in ischemic rabbit hearts. Am J Physiol Cell Physiol. 1982; 242:C288–C295.
26. Noma A. ATP-regulated K^+ channels in cardiac muscle. Nature. 1983; 305:147–149. [PubMed: 6310409]
27. Shivkumar K, Deutsch NA, Lamp ST, et al. Mechanisms of hypoxic K loss in rabbit ventricle. J Clin Invest. 1997; 100:1782–1788. [PubMed: 9312178]
28. Hartmann M, Decking U, Schrader J. Cardioprotective actions of KC 12291. II. Delaying Na+ overload in ischemia improves cardiac function and energy status in reperfusion. Arch Pharm (Weinheim). 1998; 358:554–560.
29. Ju YK, Saint DA, Gage PW. Hypoxia increases persistent sodium current in rat ventricular myocytes. J Physiol. 1996; 497:337–347. [PubMed: 8961179]
30. Kanda A, Watanabe I, Williams ML, et al. Unanticipated lessening of the rise in extracellular potassium during ischemia by pinacidil. Circulation. 1997; 95:1937–1944. [PubMed: 9107183]
31. Knopf H, Theising R, Moon CH, Hirche HJ. Continuous determination of extracellular space and changes of K, Na, Ca, and H during global ischaemia in isolated rat hearts. J Mol Cell Cardiol. 1990; 22:1259–1272. [PubMed: 2283684]
32. Morena H, Janse MJ, Fiolet AWT, et al. Comparison of the effects of regional ischemia, hypoxia, hyperkalemia, and acidosis on intracellular and extracellular potentials and metabolism in the isolated porcine heart. Circ Res. 1980; 46:634–646. [PubMed: 7363413]
33. Kodama I, Wilde A, Janse MJ, et al. Combined effects of hypoxia, hyperkalemia and acidosis on membrane action potential and excitability of guinea-pig ventricular muscle. J Mol Cell Cardiol. 1984; 16:247–259. [PubMed: 6716491]
34. Weiss JN, Venkatesh N, Lamp ST. ATP-sensitive K^+ channels and cellular K^+ loss in hypoxic and ischemic mammalian ventricle. J Physiol(Lond). 1992; 447:649–673. [PubMed: 1593462]
35. Kagiyama Y, Hill JL, Gettes LS. Interaction of acidosis and increased extracellular potassium on action potential characteristics and conduction. Circ Res. 1982; 51:614–623. [PubMed: 7139880]
36. Sato R, Noma A, Kurachi Y. Effects of intracellular acidification on membrane currents in ventricular cells of the guinea pig. Circ Res. 1985; 57:553–561. [PubMed: 2412722]

NIH-PA Author Manuscript

NIH-PA Author Manuscript

NIH-PA Author Manuscript

37. Irisawa H, Sato R. Intra- and extracellular actions of proton on the calcium current of isolated guinea pig ventricular cells. Circ Res. 1986; 59:348–355. [PubMed: 2429781]
38. Shaw R, Rudy Y. Electrophysiological effects of acute myocardial ischemia: a theoretical study of altered cell excitability and action potential duration. Cardiovasc Res. 1997; 35:256–272. [PubMed: 9349389]
39. Shaw R, Rudy Y. Electrophysiologic effects of acute myocardial ischemia. A mechanistic investigation of action potential conduction and conduction failure. Circ Res. 1997; 80:124–138. [PubMed: 8978331]
40. Kleber AG, Riegger CB, Janse MJ. Extracellular K^+ and H^+ shifts in early ischemia: mechanisms and relation to changes in impulse propagation. J Mol Cell Cardiol. 1987; 19:35–44. [PubMed: 2448490]
41. Rodríguez B, Tice B, Eason J, et al. Cardiac vulnerability to electric shocks during phase 1A of acute global ischemia. Heart Rhythm. 2004; 1:695–703. [PubMed: 15851241]
42. Rodríguez B, Tice B, Eason JC, et al. Effect of acute global ischemia on the upper limit of vulnerability. Am J Physiol. 2004; 286:H2078–H2088.
43. Downar E, Janse MJ, Durrer D. The effect of 'ischemic' blood on transmembrane potentials of normal porcine ventricular myocardium. Circulation. 1977; 55:455–462. [PubMed: 837481]
44. Kleber AG, Janse MJ, Van Capelle FJ, Durrer D. Mechanisms and time course of S-T and T-Q segment changes during acute regional myocardial ischemia in the pig heart determined by extracellular and intracellular recordings. Circ Res. 1978; 42:603–613. [PubMed: 639183]
45. Pogwizd SM, Corr PB. Electrophysiologic mechanisms underlying arrhythmias due to reperfusion of ischemic myocardium. Circulation. 1987; 76:402–426.
46. Wit, AL.; Janse, MJ. The Ventricular Arrhythmias of Ischemia and Infarction: Electrophysiological Mechanisms. Futura Publishing; Mount Kisko: 1993.
47. Ferrero JM Jr, Trenor B, Rodríguez B, Saiz J. Electrical activity and reentry during acute regional myocardial ischemia: insights from simulations. Int J Bif Chaos. 2003; 13:1–13.
48. Tice B, Rodríguez B, Trayanova N. Arrthythmogenicity of transmural heterogeneities in a realistic model of regional ischemia. Heart Rhythm. 2005; 2:S261.
49. Bernus O, Zemlin CW, Zaritsky RM, et al. Alternating conduction in the ischaemic border zone as precursor of reentrant arrhythmias: a simulation study. Europace. 2005; 7:93–104. [PubMed: 16102507]
50. Wolferth CC, Bellet S, Livezey MM, Murphy F. Negative displacement of the RS-T segment in the electrocardiogram and its relationships to positive displacement: an experimental study. Am Heart J. 1945; 29:220–244.
51. Holland RP, Brooks H. Precordial and epicardial surface potentials during myocardial ischemia in the pig: a theoretical and experimental analysis of the TQ and ST segments. Circ Res. 1975; 37:471–480. [PubMed: 1182939]
52. Li D, Li CY, Yong AC, Kilpatrick D. Source of electrocardiographic ST changes in subendocardial ischemia. Circ Res. 1998; 82:957–970. [PubMed: 9598593]
53. Johnston PR, Kilpatrick D, Li CY. The importance of anisotropy in modeling ST segment shift in subendocardial ischaemia. IEEE Trans Biomed Eng. 2001; 48:1366–1376. [PubMed: 11759918]
54. Johnston PR, Kilpatrick D. The effect of conductivity values on ST segment shift in subendocardial ischaemia. IEEE Trans Biomed Eng. 2003; 50:150–158. [PubMed: 12665028]
55. Hopenfeld B, Stinstra JG, Macleod RS. Mechanism for ST depression associated with contiguous subendocardial ischemia. J Cardiovasc Electrophysiol. 2004; 15:1200–1206. [PubMed: 15485448]
56. Hopenfeld B, Stinstra JG, Macleod RS. The effect of conductivity on ST-segment epicardial potentials arising from subendocardial ischemia. Ann Biomed Eng. 2005; 33:751–763. [PubMed: 16078615]
57. Macleod RS, Shome S, Stinstra J, et al. Mechanisms of ischemia-induced ST-segment changes. J Electrocardiol. 2005; 38(4 Suppl):8–13. [PubMed: 16226067]
58. Maclachlan MC, Sundnes J, Lines GT. Simulation of ST segment changes during subendocardial ischemia using a realistic 3-D cardiac geometry. IEEE Trans Biomed Eng. 2005; 52:799–807. [PubMed: 15887529]

NIH-PA Author Manuscript

NIH-PA Author Manuscript

NIH-PA Author Manuscript

59. Gima K, Rudy Y. Ionic current basis of electrocardiographic waveforms: a model study. Relates the electrocardiographic waveforms to cellular electrophysiological processes. Several conditions including global ischemia. Circ Res. 2002; 90:889–896. [PubMed: 11988490]
60. Aslanidi OV, Clayton RH, Lambert JL, Holden AV. Dynamical and cellular electrophysiological mechanisms of ECG changes during ischaemia. J Theor Biol. 2005; 237:369–381. [PubMed: 15979649]
61. Coronel, R. PhD Thesis. University of Amsterdam; The Netherlands: 1988. Distribution of extracellular potassium during myocardial ischemia.
62. Coronel R, Fiolet JW, et al. Distribution of extracellular potassium and its relation to electrophysiologic changes during acute myocardial ischemia in the isolated perfused porcine heart. Circulation. 1988; 77:1125–1138. [PubMed: 3359590]
63. Coronel R. Heterogeneity in extracellular potassium concentration during early myocardial ischaemia and reperfusion: implications for arrhythmogenesis. Cardiovasc Res. 1994; 28:770–777. [PubMed: 7923278]
64. Janse MJ, Cinca J, et al. The 'border zone' in myocardial ischemia. An electrophysiological, metabolic, and histochemical correlation in the pig heart. Circ Res. 1979; 44:576–588. [PubMed: 428053]
65. Walfridson H, Odman S, Lund N. Myocardial oxygen pressure across the lateral border zone after acute coronary occlusion in pig heart. Adv Exp Med Biol. 1985; 191:203–210. [PubMed: 3832843]
66. Janse MJ, Van Capelle FJL, et al. Flow of "injury current" and patterns of excitation during early ventricular arrhythmias in acute regional myocardial ischemia in isolated porcine and canine hearts. Circ Res. 1980; 47:151–165. [PubMed: 7397948]
67. Janse MJ, Kleber AG. Electrophysiological changes and ventricular arrhythmias in the early phase of regional myocardial ischemia. Circ Res. 1981; 49:1069–1081. [PubMed: 7028311]
68. Kleber AG. Conduction of the impulse in the ischemia myocardium: implications for malignant ventricular arrhythmias. Experientia. 1987; 43:1056–1061. [PubMed: 3311794]
69. Costeas C, Peters NS, Waldecker B, et al. Mechanisms causing sustained ventricular tachycardia with multiple QRS morphologies. Circulation. 1997; 96:3721–3731. [PubMed: 9396476]
70. Trenor B, Ferrero JM Jr, Rodríguez B, Montilla F. Effect of pinacidil on reentrant arrhythmias generated during acute myocardial ischemia. Ann Biomed Eng. 2005; 33:897–906. [PubMed: 16060529]
71. Wilkensky RL, Tranum-Jensen J, et al. The subendocardial border zone during acute ischemia of the rabbit heart: an electrophysiologic, metabolic and morphologic correlative study. Circulation. 1986; 74:1137–1146. [PubMed: 3769171]
72. Hill JL, Gettes LS. Effect of acute coronary artery occlusion on local myocardial extracellular K^+ activity in swine. Circulation. 1980; 61:768–778. [PubMed: 7357719]
73. Gilmour RF Jr, Zipes DP. Different electrophysiological responses of canine endocardium and epicardium to combined hyperkalemia, hypoxia, and acidosis. Circ Res. 1980; 46:814–825. [PubMed: 7379247]
74. Kimura S, Bassett AL, Kohya T, et al. Simultaneous recording of action potentials from endocardium and epicardium during ischemia in the isolated cat ventricle: relation of temporal electrophysiologic heterogeneities to arrhythmias. Circulation. 1986; 74:401–409. [PubMed: 3731429]
75. Schaapherder AFM, Schumacher CA, Coronel R, Fiolet JWT. Transmural heterogeneity of extracellular [K^+] and pH and myocardial energy metabolism in the isolated rat heart during acute global ischemia; dependence on gaseous environment. Bas Res Cardiol. 1990; 85:33–44.
76. Furukawa T, Kimura S, Furukawa N, et al. Role of cardiac ATP-regulated potassium channels in differential responses of endocardial and epicardial cells to ischemia. Circ Res. 1991; 68:1693–1702. [PubMed: 2036719]
77. Behrens S, Li C, Franz MR. Effects of myocardial ischemia on ventricular fibrillation inducibility and defibrillation efficacy. J Am Coll Cardiol. 1997; 29:817–824. [PubMed: 9091529]
78. Chen PS, Shibata N, Dixon EG, et al. Comparison of the defibrillation threshold and the upper limit of ventricular vulnerability. Circulation. 1986; 73:1022–1028. [PubMed: 3698224]

NIH-PA Author Manuscript

NIH-PA Author Manuscript

NIH-PA Author Manuscript

79. Hwang C, Swerdlow CD, Kass RM, et al. Upper limit of vulnerability reliably predicts the defibrillation threshold in humans. Circulation. 1994; 90:2308–2314. [PubMed: 7955188]
80. Efimov IR, Cheng Y, et al. Virtual electrode-induced phase singularity: a basic mechanism of defibrillation failure. Circ Res. 1998; 82:918–925. [PubMed: 9576111]
81. Rodríguez B, Li L, Eason JC, et al. Differences between left and right ventricular chamber geometry affect cardiac vulnerability to electric shocks. Circ Res. 2005; 97:168–175. [PubMed: 15976315]
82. Trayanova N. Concepts of ventricular defibrillation. Phil Trans Roy Soc Lond. 2001; 359:1327–1337.
83. Skouibine K, Trayanova NA, Moore P. Success and failure of the defibrillation shock: insights from a simulation study. J Cardiovasc Electrophysiol. 2000; 11:785–796. [PubMed: 10921796]
84. Trayanova NA, Eason JC, Aguel F. Computer simulations of cardiac defibrillation: A look inside the heart. Comput Visual Sci. 2002; 4:259–270.
85. Rodríguez B, Trayanova N. Upper limit of vulnerability in a defibrillation model of the rabbit ventricles. J Electrocardiol. 2003; 36(Suppl):51–56. [PubMed: 14716592]
86. Trayanova, N.; Aguel, F.; Larson, C.; Haro, C. Modeling cardiac defibrillation: an inquiry into post-shock dynamics. In: Zipes, DP.; Jalife, J., editors. Cardiac Electrophysiology: From Cell to Bedside. 4. W.B. Saunders; Philadelphia: 2004. p. 282-291.
87. Plonsey R. The use of a bidomain model for the study of excitable media. Lec Math Life Sci. 1989; 21:123–149.
88. Wikswo JP Jr, Lin SF, Abbas RA. Virtual electrodes in cardiac tissue: a common mechanism for anodal and cathodal stimulation. Biophys J. 1995; 69:2195–2210. [PubMed: 8599628]
89. Efimov IR, Cheng Y, Van Wagoner DR, et al. Virtual electrode-induced phase singularity: a basic mechanism of defibrillation failure. Circ Res. 1998; 82:918–925. [PubMed: 9576111]
90. Cheng Y, Mowrey KA, et al. Mechanisms of shock-induced arrhythmogenesis during acute global ischemia. Am J Physiol Heart Circ Physiol. 2002; 282:H2141–H2151. [PubMed: 12003822]
91. Cheng Y, Mowrey KA, Van Wagoner DR, et al. Virtual electrode-induced reexcitation: a mechanism of defibrillation. Circ Res. 1999; 85:1056–1066. [PubMed: 10571537]
92. Efimov IR, Aguel F, Cheng Y, et al. Virtual electrode polarization in the far field: implications for external defibrillation. Am J Physiol Heart Circ Physiol. 2000; 279:H1055–H1070. [PubMed: 10993768]
93. Evans FG, Ideker RE, Gray RA. Effect of shock-induced changes in transmembrane potential on reentrant waves and outcome during cardioversion of isolated rabbit hearts. J Cardiovasc Electrophysiol. 2002; 13:1118–1127. [PubMed: 12475103]
94. Lindblom AE, Aguel F, Trayanova NA. Virtual electrode polarization leads to reentry in the far field. J Cardiovasc Electrophysiol. 2001; 12:946–956. [PubMed: 11513448]
95. Roth BJ. An S1 gradient of refractoriness is not essential for reentry induction by an S2 stimulus. IEEE Trans Biomed Eng. 2000; 47:820–821. [PubMed: 10833857]
96. Rodríguez B, Tice BM, Blake R, et al. Vulnerability to electric shocks in regional ischemia. Heart Rhythm Abstract. 2006; 3(5):5226.

NIH-PA Author Manuscript

NIH-PA Author Manuscript

NIH-PA Author Manuscript

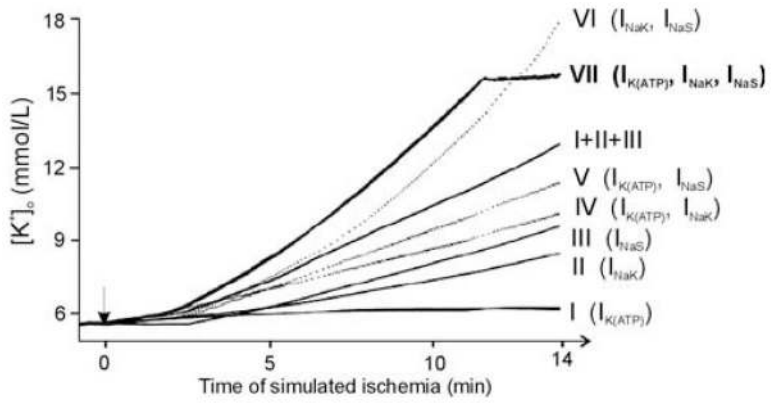

FIGURE 1.

Time courses of the extracellular K^+ concentration ($[K^+]_o$) during 14 min of ischemia obtained for different ischemic mechanisms. Traces I–III represent individual effects on $[K+]_o$ of: change in ATP-sensitive K^+ current ($I_{K(ATP)}$); current through the Na^+/K^+ pump (I_{NaK}); and inclusion of ischemia-activated Na^+ inward current (I_{NaS}), respectively. Trace "I + II + III" is the sum of traces I–III. Traces IV–VI correspond to the combined effect of the two mechanisms indicated next to each trace. Trace VII depicts the simultaneous effect of the three mechanisms on $[K^+]_o$. In all cases, when $I_{K(ATP)}$ was activated, the final value of the fraction of activated ATP-sensitive K^+ (K_{ATP}) channels was 0.8%. When I_{NaS} was activated, the final value of I_{NaS} was 1.2 μA/μF, and when an inhibition of the maximum current through the Na^+/K^+ pump was considered, the final value of the degree of inhibition of the Na^+/K^+ was 35%. (Modified from reference 13.)

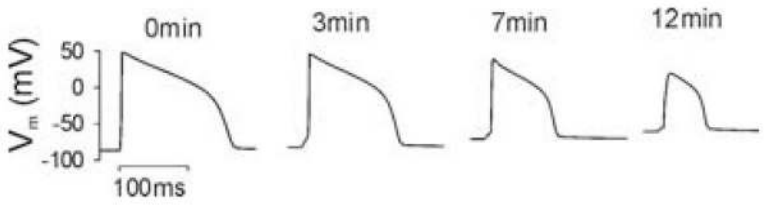

FIGURE 2.
Evolution of the action potential during 12 min of simulated ischemia.

NIH-PA Author Manuscript
NIH-PA Author Manuscript
NIH-PA Author Manuscript

NIH-PA Author Manuscript

NIH-PA Author Manuscript

NIH-PA Author Manuscript

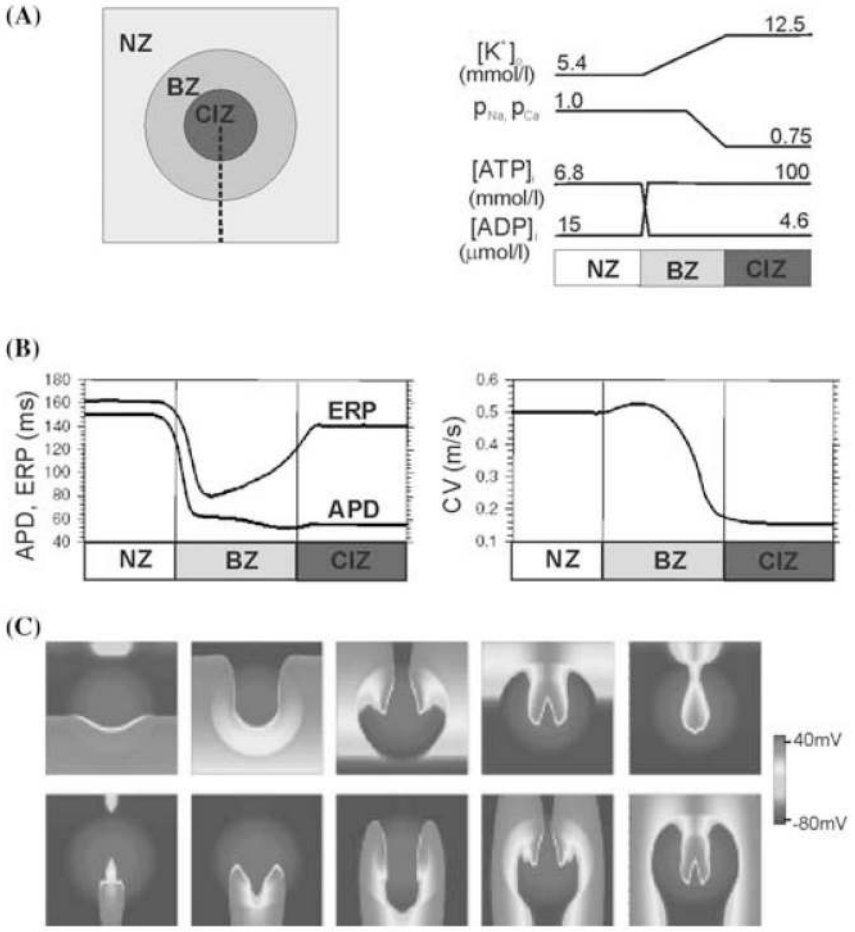

FIGURE 3.

Arrhythmogenesis in regional ischemia. Panel **A:** Schematic of the 2D model of regionally ischemic tissue (left) and the spatial variations in extracellular potassium concentration ($[K^+]_o$), intracellular ATP and ADP concentrations ($[ATP]_i$ and $[ADP]_i$), and the degree of inhibition of the maximum conductances of the Na^+ and Ca^{2+} currents in the central ischemic zone (CIZ), border zone (BZ), and normal zone (NZ) (right). Panel **B:** Spatial variation in the effective refractory period and action potential duration (left) and in the longitudinal conduction velocity (right) along the dashed line depicted in panel **A**, left. Panel **C:** Snapshots of transmembrane potential distribution at different instants of time following the delivery of a premature stimulus at CI = 210 msec in the lower part of the 2D sheet illustrated in panel **A.** Snapshots are separated by 50 msec; the first corresponds to 50 msec after the delivery of the premature stimulus. Panel C is shown in color online. (Modified from reference 47.)

NIH-PA Author Manuscript

NIH-PA Author Manuscript

NIH-PA Author Manuscript

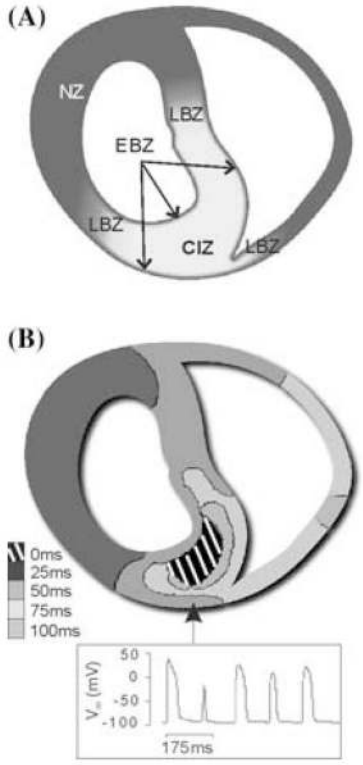

FIGURE 4.

Contribution of transmural heterogeneities to arrhythmogenesis in regional ischemia. Panel **A:** 2D anatomically accurate rabbit ventricular model of regional ischemia following LAD occlusion. CIZ is central ischemia zone, NZ–normal zone, EBZ–endo and epicardial border zone, and LBZ–lateral border zone. Panel **B:** Activation time map of a reentrant beat following a premature stimulus (top) and time course of transmembrane potential in the node marked by the arrow (bottom). (Modified from reference.[48])

NIH-PA Author Manuscript

NIH-PA Author Manuscript

NIH-PA Author Manuscript

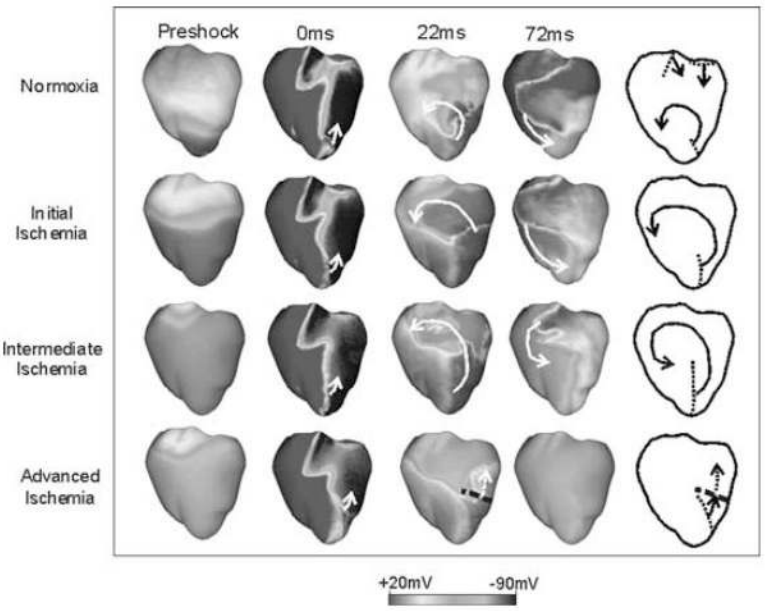

FIGURE 5.

Anterior transmembrane potential distribution in normoxia and global ischemia for a 6.4 V/cm shock applied at CI = 160 msec. Times refer to shock end. Color scale is saturated, that is, potentials above +20 mV and below −90 mV appear red and blue, respectively. Diagrams present major features of postshock behavior. Dotted lines indicate spatial extent of wavefronts at shock end. Solid arrows show direction of propagation. Dashed arrows depict direction of decremental conduction. Thick dashed lines mark locations at which conduction becomes decremental. The Figure is shown in color online. (Modified from reference 40.)